

- (b) Woods, G. B.; Panagiotopoulos, A. Z.; Rowlinson, J. S. *Mol. Phys.* **1988**, *63*, 49. (c) Baksh, M. S. A.; Yang, R. T. *AIChE J.* **1991**, *37*, 923. (d) Cracknell, R. F.; Gordon, P.; Gubbins, K. E. *J. Phys. Chem.* **1993**, *97*, 494. (e) Suh, S.-H.; Park, H.-K. *Korean J. Chem. Eng.* **1994**, *11*, 198.
4. (a) Yashonath, S.; Demontis, P.; Klein, M. L. *Chem. Phys. Lett.* **1988**, *153*, 551. (b) Woods, G. B.; Rowlinson, J. S. *J. Chem. Soc. Faraday Trans. 2* **1989**, *85*, 765. (c) Rasmus, D. M.; Hall, C. K. *AIChE J.* **1991**, *37*, 769. (d) Snurr, R. Q.; June, R. L.; Bell, A. T.; Theodorou, D. N. *Mol. Simul.* **1991**, *8*, 73. (e) Santikary, P.; Yashonath, S. *J. Chem. Soc. Faraday Trans.* **1992**, *88*, 1063. (f) Cracknell, R. F.; Gubbins, K. E. *Langmuir* **1993**, *9*, 824. (g) Van Tassel, P. R.; Davis, H. T.; McCormick, A. V. *J. Chem. Phys.* **1993**, *98*, 8919. (h) Jameson, C. J.; Jameson, A. K.; Baello, B. I.; Lim, H.-M. *J. Chem. Phys.* **1994**, *100*, 5965.
5. Nicholson, D.; Parsonage, N. G. In *Computer Simulation and the Statistical Mechanics of Adsorption*; Academic Press: New York, 1982; Chap. 5.
6. Szostak, R. In *Handbook of Molecular Sieves*; Van Nostrand Reinhold: New York, 1992.
7. Lee, L. L. In *Molecular Thermodynamics of Nonideal Fluids*; Butterworth Publishers: London, 1988; Chap. 9.
8. (a) Adams, D. J. *Mol. Phys.* **1974**, *28*, 1241. (b) *ibid.* **1975**, *29*, 307.
9. (a) MacElroy, J. M. D.; Suh, S.-H. *AIChE Symp. Ser.* **1986**, *82*, 133. (b) MacElroy, J. M. D.; Suh, S.-H. *Mol. Phys.* **1987**, *60*, 475. (c) MacElroy, J. M. D.; Suh, S.-H. *Mol. Simul.* **1989**, *2*, 313. (d) Suh, S.-H.; Kim, J.-S.; Park, C.-Y. *Hwahak Konghak* **1991**, *29*, 742.
10. Miller, G. W.; Knaebel, K. S.; Ikels, K. G. *AIChE J.* **1987**, *33*, 194.
11. (a) McCormick, A. V.; Chmelka, B. F. *Mol. Phys.* **1991**, *73*, 603. (b) Cohen de Lara, E.; Seloudoux, R. *J. Chem. Soc. Faraday Trans. 1* **1983**, *79*, 2271.

A Theoretical Investigation of the CO Adsorption on Cobalt Surfaces: Co(0001), (10 $\bar{1}$ 0), (11 $\bar{2}$ 0), and (10 $\bar{1}$ 2)

Yon-Tae Je* and Audrey L. Companion

*Department of Chemistry, Gyeongsang National University, Chinju 660-701, Korea

Department of Chemistry, University of Kentucky, Lexington, KY 40506, U.S.A.

Received February 24, 1995

Binding characteristics of single CO molecules adsorbed on cobalt surfaces: Co(0001), (10 $\bar{1}$ 0), (11 $\bar{2}$ 0), and (10 $\bar{1}$ 2) were investigated theoretically employing the semi-empirical ASE-MO method to help better understand the mechanism of CO dissociation on these cobalt surfaces. On all these surfaces, there were observed gradual increases in optimum C-O and Co-C distances (d_{C-O} and d_{Co-C}) and the consequent decreases in C-O and Co-C bond orders (p_{C-O} and p_{Co-C}), and small increases in binding energy (BE) and relative stability of CO to the surface as the binding site of CO changes from on-top to 2-fold bridge and/or to 3-fold bridge (or hollow) site on a given specific layer, the same trend in most calculation works. For such site change of CO, stretching C-O vibrational frequencies (ν_{C-O}) decreased significantly on all cobalt crystal surfaces and the corresponding cobalt-C stretching frequencies (ν_{Co-C}) also dropped, but not as strongly as the ν_{C-O} . For example, from a CO on the (0001), ν_{C-O} decreases from 1969-1992 cm^{-1} for on-top to 1693-1763 cm^{-1} for 2-fold bridge and then to 1560-1635 cm^{-1} for 3-fold hollow site CO species and their ν_{Co-C} declines from 569-590 cm^{-1} to 472-508 cm^{-1} and then to 470-482 cm^{-1} . In addition, atomic C-Co stretching frequencies were computed as a possible aid in a future experiment.

Introduction

Transition metals have been paid a significant amount of attention through several decades as catalysts for hydrocarbon synthesis reactions such as the Fischer-Tropsch reaction; the catalytic conversion of synthesis gas (CO and H₂) to chain hydrocarbons.^{1,2} It was widely admitted that the first step in Fischer-Tropsch processes is the dissociation of CO molecules on a metal surface to form mainly surface carbidic (rather than graphitic) carbon and oxygen, then followed by the hydrogenation of carbidic carbon to form hydrocarbons.^{3,4} In order to help better understand the mechanism of this CO dissociation on metal surfaces, there have been numer-

ous studies on the surface structure and binding sites of carbon monoxide on surfaces of several transition metals such as nickel, iron, platinum, and ruthenium.

Here are abstracted some distinguished experimental and theoretical achievements from those studies. The interaction between CO and metal surface has been portrayed traditionally by the Blyholder model,⁵ in which bonding in a metal-carbonyl complex is depicted by the CO 5 σ to metal forward donation and metal d to CO 2 π^* back-donation, with some support⁶ and criticism⁷ later. Several experimental and theoretical studies indicated that CO adsorbs (or binds) in the end-on orientation with the carbon-end toward a metal surface for transition metals in the right-side of the periodic

table,^{8,9} while evidence of the side-on (lying-down or tilted) orientation for the early left-side transition metals has also been reported.^{10,11} There is an agreement that CO can bind to a metal surface by discrete binding sites: on-top (or linear), 2-fold, 3-fold, and/or 4-fold bridge site and that a given site on a given crystal plane will possess the typical vibrational frequency of a narrow range and that the frequency ranges for different sites will not seriously overlap each other.¹² There has been also abundant body of evidence that a single crystalline surface can accommodate several CO binding sites, depending on the CO coverage, yielding characteristic vibrational frequencies.^{13,14}

However, not many studies of this line have been fulfilled for CO molecules on a cobalt metal despite of the same degree of significance of this metal in the Fischer-Tropsch reaction; only a few experiments reported with no theoretical work up to recently. For example, it has long been known that Co metal produces a mixture of short and long chain hydrocarbons while Ni yields methane uniquely.¹⁵ This shortage of experimental work on cobalt seems partly due to the problem in preparing clean crystal planes of a cobalt metal. This comes mainly from the phase transition from hcp (hexagonal close-packed) to fcc (face-centered cubic) structure taking place around 700 K, very low compared to ordinary high temperatures in the UHV system necessary to remove common contaminants, such as carbon and oxygen, from the metal surface.

We report in this paper the results from a theoretical investigation, applying the semi-empirical ASED-MO method, of the binding structure and energetics and the vibrational frequencies for single CO molecules adsorbed on single crystalline planes of a cobalt metal; Co(0001), (10 $\bar{1}$ 0), (11 $\bar{2}$ 0), and (10 $\bar{1}$ 2), as a leading study for the interaction (mainly CO dissociation and carbon aggregation) of CO species on these cobalt surfaces which will be reported in a separate paper.

Methods

MO Calculation. Molecular orbital calculations were carried out with the ASED-MO method developed by A. B. Anderson^{16,17} as a modified version of the EHMO method. It has been used with much success in several semi-empirical MO calculations. There are known two major modifications in ASED-MO: (1) the total molecular energy is expressed as a sum of the two-body repulsive energy term due to atom-atom pairwise electrostatic interaction and the attractive energy term due to electronic delocalization as atoms come together to form a molecule; (2) the Wolfsberg-Helmholtz constant, K , is replaced by a distance-dependent exponential term leading to improved equilibrium distances and vibrational potential functions. The particular computer program used in this paper is a modified version called ASE-DGE¹⁸ which contains a multi-parameter pattern search optimization facility. This allows rapid searching for either minimum or maximum energy while changing any or all of the cartesian coordinates for a selected number of atoms.

Vibrational Frequency Analysis. The fundamental stretching C-O and Co-C vibrational frequencies were calculated using the direct vibrational analysis method. This is a simple method to directly calculate vibrational frequencies of atomic or molecular species on a metal surface. The

Table 1. The set of ASED-MO input parameters for C, O, and Co atoms used in this study

Atom	Orbital	VSIE (eV)	C_1	ζ_1	C_2	ζ_2
C	2s	-20.00	-	1.658	-	-
	2p	-11.03	-	1.618	-	-
O	2s	-28.48	-	2.246	-	-
	2p	-13.35	-	2.227	-	-
Co	4s	-8.70	-	1.75	-	-
	4p	-5.25	-	1.45	-	-
	3d	-11.21	0.555	1.55	0.646	1.900

VSIE=valence state ionization energy of atomic orbital; ζ_1 & ζ_2 =Slater exponents for atomic orbital in a.u.; C_1 & C_2 =double zeta coefficients for cobalt 3d orbital.

Table 2. The ASED-MO calculated and the corresponding experimental values for a free (unadsorbed) CO molecule

	dC-O (Å)	DE (eV)	μ (D)	ν C-O (cm ⁻¹)
ASED-MO calc.	1.1165	9.03	0.126	2150
Experimental	1.128	11.23	0.13	2143

dC-O, DE, μ , and ν C-O are C-O bond distance, bond dissociation energy, dipole moment, and fundamental stretching C-O vibrational frequency, respectively.

theory was first introduced by Huff and Ellison,¹⁹ and has been programmed for a personal computer and successfully applied to a recent work by Maruca *et al.*¹⁴

Modeling and Parameterization. The experimental bond distance, bond dissociation energy, and stretching C-O vibrational frequency for a gaseous free (unadsorbed) CO molecule are 1.128 Å, 11.23 eV, and 2143 cm⁻¹ respectively from spectroscopic sources.²⁰⁻²² The experimental dipole moment is measured as 0.13 Debye.²³ The set of ASED input atom parameters for C and O (Table 1) adopted in our study was from Maruca *et al.*¹⁴ and with this set the ASED computed values for free CO matched closely the corresponding experimental values as shown in Table 2.

Cobalt metal possesses a hexagonal close-packed (hcp) structure below 700 K. The distance between nearest Co atoms (in contact) is 2.51 Å from crystallographic data²⁴ and the cohesive energy for cobalt metal is measured as 4.39 eV/atom.²⁵ Cobalt cluster surfaces of the common (0001) crystal plane (see Figure 1) were created (simulated) on a terminal of the IBM 3090-600E supercomputer (at the University of Kentucky Computing Center) with assorted cluster sizes (2-50 Co atoms and 1-3 layers). The ASED-MO input parameters for Co atom were searched, tested, and slightly modified until the calculated cohesive energy of a cobalt cluster of an appropriate size resembled closely the experimental cohesive energy, 4.39 eV/atom. The valence-state ionization energy of cobalt 3d orbitals, VSIE_{3d} (eV), was further modified so that the calculated C-O stretching frequency of a CO (by on-top site) on the Co₅₀(0001) surface matched the observed C-O stretching frequency value, 1990 cm⁻¹, from a recent experiment on the Co(0001) surface by Geerlings

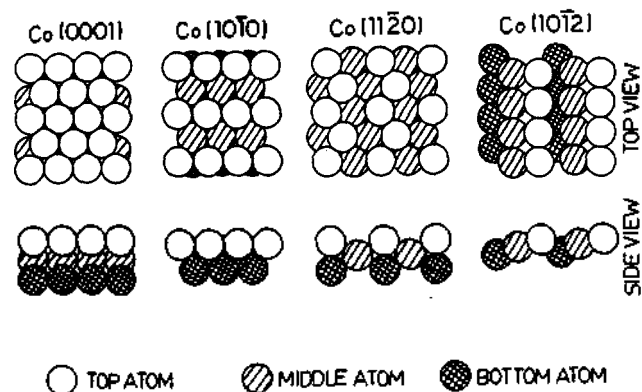


Figure 1. Integrated representation of four cobalt surfaces; Co (0001), (10 $\bar{1}$ 0), (11 $\bar{2}$ 0) and (10 $\bar{1}$ 2).

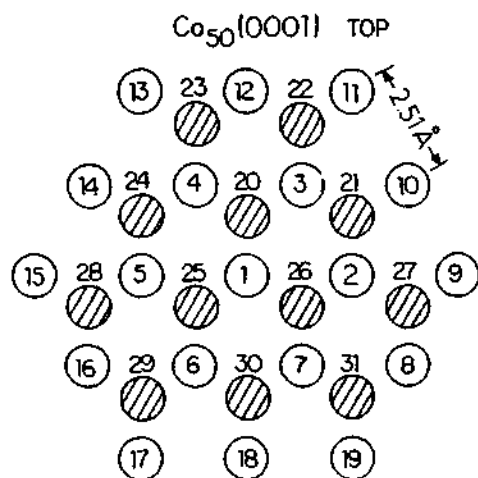


Figure 2. Top view of the $\text{Co}_{50}(0001)$ cluster with lattices expanded. Empty and shaded circles represent Co atoms of top and middle layer, each. Bottom layer is the repeated top layer 4.0988 Å below (invisible). Layer-layer separations for top-middle and middle-bottom are 2.0494 Å and 2.0494 Å, each.

*et al.*²⁶ Table 1 lists the set of ASED-MO input parameters for C, O, and Co atoms which were used in this paper.

Cobalt surfaces representing four different crystalline planes: (0001), (10 $\bar{1}$ 0), (11 $\bar{2}$ 0), and (10 $\bar{1}$ 2) are drawn in Figures 1, 2, 3, 4, and 5. Figure 1 integrates these four cobalt surfaces to afford a better view of their features in close-packed arrays. Lattices are expanded in Figures 2, 3, 4, and 5 to clearly show the relative locations of all Co atoms. Each Co atom is numbered (for computation) and typical Co-Co distances are indicated. Layer-layer separations are given in the paragraph below the picture. The $\text{Co}_{50}(0001)$ cluster surface (in Figure 2), commonly called "smooth" surface, was created with 50 Co atoms in 3 layers. The $\text{Co}_{43}(10\bar{1}0)$ surface (in Figure 3) consisted of 43 atoms in 3 layers. The $\text{Co}_{49}(11\bar{2}0)$ surface, of 49 atoms in 3 layers, features the arrangement of Co atoms forming zigzag troughs (see Figures 4 and 1) and so is called "zigzag" surface. The $\text{Co}_{47}(10\bar{1}2)$ (Figure 5), of 47 atoms in 3 layers, has a side view of parallel step-like arrays and often referred to "stepped" surface (see

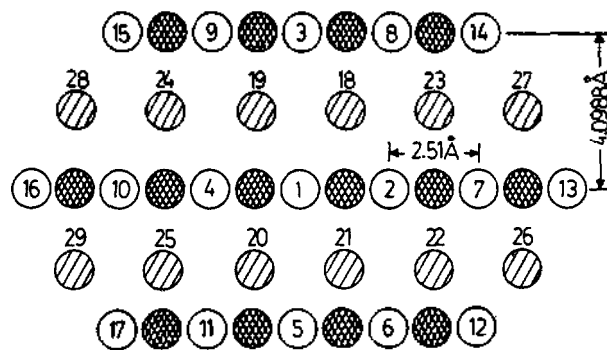


Figure 3. Top view of the $\text{Co}_{43}(10\bar{1}0)$ cluster with lattices expanded. Empty, less-shaded, and more-shaded circles represent Co atoms of top, middle, and bottom layer, each. Layer-layer separations for top-middle and middle-bottom are 0.7246 Å and 1.4491 Å, each.

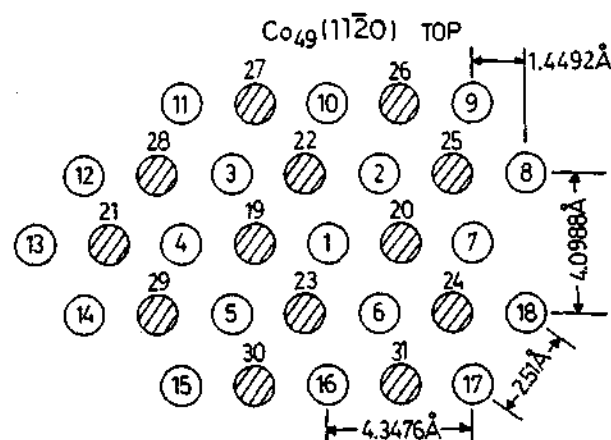


Figure 4. Top view of the $\text{Co}_{49}(11\bar{2}0)$ cluster with lattices expanded. Empty and shaded circles represent Co atoms of top and middle layer, each. Bottom layer is the repeated top layer 2.5100 Å below (invisible). Layer-layer separations for top-middle and middle-bottom are 1.255 Å and 1.255 Å, each.

Figure 1, too).

There will be seen, in the following tables, small variations in the calculated values, such as binding energy and vibrational C-O and Co-C stretching frequencies, among different binding positions for a specific site of a CO on each layer of each cobalt surface. However, this (size or edge effect) is purely due to the finite size of a cobalt cluster and insignificant since it would all disappear if the cluster were infinite in its size.

Results and Discussion

Binding Structure and Energetics

CO Binding on Co(0001). Three different binding sites are possible for the adsorption of CO molecule on the smooth $\text{Co}_{50}(0001)$ cluster surface (Figure 2); on-top (or linear), 2-fold bridge, and 3-fold bridge (or hollow) site on the top layer, all with the C-O axis perpendicular to a metal surface. Each of these CO binding sites is drawn in Figure

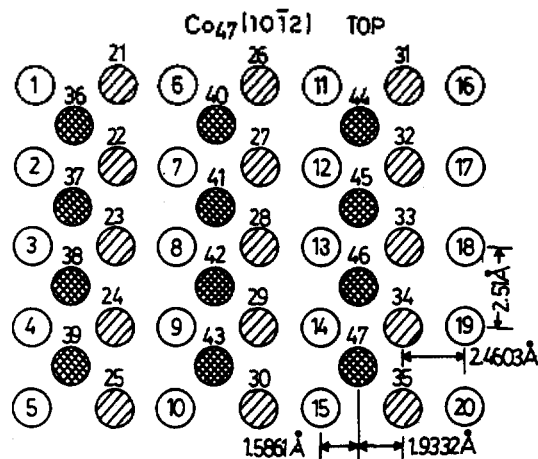


Figure 5. Top view of the $\text{Co}_{47}(10\bar{1}2)$ cluster with lattices expanded. Empty, less-shaded, and more-shaded circles represent Co atoms of top, middle, and bottom layer, each. Layer-layer separations for top-middle and middle-bottom are 0.4970 \AA and 1.4912 \AA , each.

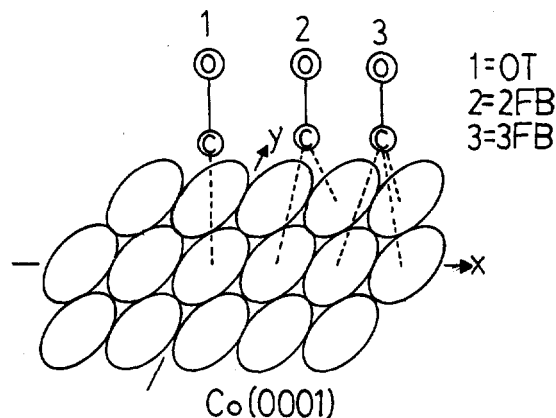


Figure 6. Visual representation of three CO binding sites on a $\text{Co}(0001)$ surface. OT, 2FB, and 3FB represent on-top, 2-fold bridge, and 3-fold bridge (or hollow) site, respectively.

6 as an exemplary display; OT, 2FB, and 3FB indicate on-top, 2-fold bridge, and 3-fold bridge site, respectively. The ASE-D-MO calculation (geometry optimization) results for single CO molecules adsorbed on this $\text{Co}(0001)$ surface by these different sites (and positions) are tabulated in Table 3.

C-O and Co-C distances ($d\text{C-O}$ and $d\text{Co-C}$) listed were obtained by optimizing C and O atoms in the z direction (normal to the surface). All Co atoms were assumed as fixed. Overlap populations (indicative of bond orders) between carbon and oxygen ($p\text{C-O}$) and between carbon and individual Co atoms ($p\text{Co-C}$) were computed from their optimum C-O and Co-C distances. The $p\text{Co-C}$ values listed are for single Co-C bonds and so are averages of two (for 2-fold bridges) or three (for 3-fold hollows) individual values in case of multiple bridge CO site. Binding energy (BE) of a CO to the cluster surface by each site & position was calculated by subtracting the energy of a free (unadsorbed) CO and the energy of the cluster itself from the energy of the adsorbate system, $\text{CO}/\text{Co}_{50}(0001)$. Stretching C-O and Co-C vibrational

Table 3. The results from CO on $\text{Co}_{50}(0001)$ cluster surface

Site & position	$d\text{C-O}$ (\AA)	$d\text{Co-C}$ (\AA)	$p\text{C-O}$	$p\text{Co-C}$	BE (eV)	$\nu\text{C-O}$ (cm^{-1})	$\nu\text{Co-C}$ (cm^{-1})
T(1Y)	1.107	1.746	1.55	0.87	-3.32	1992	594
T(2Y)	1.108	1.748	1.54	0.85	-3.28	1986	592
T(9Y)	1.110	1.754	1.52	0.84	-2.96	1969	582
T(12Y)	1.109	1.751	1.53	0.84	-3.09	1975	587
B(1,2Y)	1.129	1.872	1.45	0.50	-3.82	1693	508
B(2,10Y)	1.125	1.881	1.47	0.48	-3.48	1744	499
B(10,11Y)	1.123	1.880	1.47	0.47	-3.32	1763	492
B(11,12Y)	1.125	1.881	1.47	0.48	-3.49	1751	495
H(1,2,3Y)	1.136	1.941	1.42	0.36	-4.09	1597	480
H(1,3,4Y)	1.140	1.936	1.41	0.36	-4.04	1560	482
H(2,3,10Y)	1.139	1.942	1.41	0.35	-3.85	1587	480
H(3,11,12Y)	1.134	1.946	1.43	0.34	-3.73	1635	470

$d\text{C-O}$ & $d\text{Co-C}=\text{C-O}$ & Co-C distances; $p\text{C-O}$ & $p\text{Co-C}=\text{C-O}$ & single Co-C bond orders; BE=binding energy; $\nu\text{C-O}$ & $\nu\text{Co-C}=\text{C-O}$ & Co-C stretching frequencies; T=on-top, B=2-fold bridge, H=3-fold hollow site; Numbers in parenthesis indicate Co atoms involved in each site and position; Superscripted t=on top layer.

frequencies ($\nu\text{C-O}$ and $\nu\text{Co-C}$) are also listed in Table 3 and discussed later.

Both C-O and Co-C distances ($d\text{C-O}$ and $d\text{Co-C}$) increase gradually as the CO binding site changes from on-top to 2-fold bridge and then to 3-fold hollow site, while their C-O and Co-C bond orders ($p\text{C-O}$ and $p\text{Co-C}$) show the opposite trend (steady decrease) as predicted (since bond order is in the reverse relationship to bond length). Specifically, $d\text{C-O}$ increases from $1.107\text{-}1.110 \text{ \AA}$ for on-top to $1.123\text{-}1.129 \text{ \AA}$ for 2-fold bridge and then to $1.134\text{-}1.140 \text{ \AA}$ for 3-fold hollow site with the consequent drops in the $p\text{C-O}$ from $1.52\text{-}1.55$ to $1.45\text{-}1.47$ and then to $1.41\text{-}1.43$. The $d\text{Co-C}$ also increases from $1.746\text{-}1.754 \text{ \AA}$ to $1.872\text{-}1.881 \text{ \AA}$ and then to $1.936\text{-}1.946 \text{ \AA}$ for such site shift with the ensuing drops in the $p\text{Co-C}$ from $0.84\text{-}0.87$ to $0.47\text{-}0.50$ and to $0.34\text{-}0.36$. The degree of these changes in the $d\text{Co-C}$ and $p\text{Co-C}$ is somewhat larger than that in the $d\text{C-O}$ and $p\text{C-O}$.

Calculated binding energies (BE) indicate that single CO molecules are more strongly bound to multiple sites of the (0001) surface. Considering that as a CO binds (adsorbs) more strongly to the surface, it is more stabilized; it is seen that 3-fold hollow CO species become most stable (with BE values= $3.73\text{-}4.09 \text{ eV}$), 2-fold bridge species next most stable (BE= $3.32\text{-}3.82 \text{ eV}$) and on-top ones least stable (BE= $2.96\text{-}3.32 \text{ eV}$), the same trend in other calculation works.^{14,27,28} These larger BE values of single CO's by multiple sites seem related directly to their larger total $p\text{Co-C}$ values, which are obtained by multiplying each individual $p\text{Co-C}$ value by 2 for 2-fold bridge, or 3 for 3-fold hollow site species.

Our calculated binding energies of CO on the $\text{Co}(0001)$ were close to the ASE-D-MO calculation results of CO on a $\text{Ni}_{13}(111)$ surface,¹⁴ whose structural feature is similar to the $\text{Co}(0001)$, (BE on the $\text{Ni}(111)$ was computed as $2.73\text{-}2.87 \text{ eV}$ for on-top, $3.28\text{-}3.39 \text{ eV}$ for 2-fold bridge, and $3.41\text{-}3.66$

Table 4. Typical charges developed on carbon and oxygen of CO adsorbed on cobalt surfaces

		Planes			
		(0001)	(10 $\bar{1}0$)	(11 $\bar{2}0$)	(10 $\bar{1}2$)
On-top	C	+0.19	+0.19	+0.20	+0.26
	O	-0.27	-0.29	-0.29	-0.23
Bridge	C	+0.10	+0.14	+0.12	+0.18
	O	-0.51	-0.42	-0.46	-0.42
Hollow	C	+0.07	-	-	-
	O	-0.58	-	-	-

On-top=on-top site; Bridge=2-fold bridge site; Hollow; 3-fold hollow site.

eV for 3-fold bridge species). However, these ASED calculated BE values were estimated somewhat larger than experimental ones. For example, the isosteric heat of adsorption of CO molecules on a Co(0001) was measured in an experiment by Papp²⁹ as 1.33 eV up to CO coverage (θ_{CO}) of 0.3 and 1.00 eV for $\theta_{CO} > 0.3$. Also, experimentally measured BE's for CO on Ni(111), (110), and (100) are in the range of 1.0 to 2.0 eV.¹⁴ The cause for these larger BE values in the ASED is not clear at the present, but seems to be partly due to repulsive interactions between nearby CO species, which are not considered in the present calculation of single CO's. That is, neighboring CO species at high coverage would interact appreciably with each other mainly in a repulsive way and decrease binding energies as also demonstrated in Papp's experiment²⁹ above.

In fact, there has been some experimental evidence^{13,30} that the relative stability of adsorbed CO's depends on the CO coverage on a metal surface; that is, at low coverage, hollow site CO species become most stable, but, as the coverage increases, 2-fold bridge and then, in turn, on-top CO species become the most stable. Maruca *et al.*¹⁴ explained this experimental observation by examining the atomic charge distribution on C and O of adsorbed CO in a calculation work for CO on Ni surfaces. That is, whereas the absolute magnitude of atomic charges computed by ASED-MO may be too high, the trend is that CO molecules become more highly and negatively charged from on-top to 2-fold bridge and then to hollow site CO binding. Thus, CO molecules bound to hollow sites should repel each other more than those bound to bridge sites, and then, in turn, those to on-top sites, and become the least stable at high CO coverages with reduced binding energies. Similarly, atomic charges distributed on C and O atoms of single CO's on Co surfaces in this work lead to more highly and negatively charged hollow site CO, as shown in Table 4, which will turn least stable at high coverage. For example, typical atomic charges developed on carbon and oxygen of CO on the (0001) surface were: +0.19, +0.10, and +0.07 on the C atom, and -0.27, -0.44, and -0.55 on the O atom for on-top, bridge, and hollow CO species, respectively.

By a careful examination, there are recognized two different hollow sites on the (0001); for example, the hollow (1,3,4)' site of having a middle layer Co atom under it, and the hollow (1,2,3)' site with no such Co atom underneath. How-

Table 5. The results from CO on Co₄₃(10 $\bar{1}0$) cluster surface

Site & position	dC-O (Å)	dCo-C (Å)	pC-O	pCo-C	BE (eV)	vC-O (cm ⁻¹)	vCo-C (cm ⁻¹)
T(1) ^y	1.112	1.744	1.51	0.86	-3.48	1923	598
T(2) ^y	1.112	1.745	1.51	0.86	-3.47	1920	595
T(3) ^y	1.110	1.751	1.52	0.82	-3.39	1949	586
T(13) ^y	1.111	1.754	1.52	0.81	-3.14	1954	583
T(18) ^m	1.101	1.770	1.58	0.83	-3.26	2057	574
T(27) ^m	1.106	1.765	1.55	0.84	-3.15	2014	577
B(1,2) ^y	1.122	1.882	1.48	0.47	-3.88	1756	493
B(7,13) ^y	1.122	1.887	1.48	0.46	-3.50	1777	490
B(8,14) ^y	1.122	1.886	1.48	0.45	-3.57	1772	489
B(18,19) ^m	1.132	1.924	1.45	0.52	-3.97	1677	470
B(18,23) ^m	1.131	1.924	1.45	0.51	-3.99	1678	468
B(23,27) ^m	1.130	1.932	1.46	0.49	-3.73	1698	458

dC-O & dCo-C=C-O & Co-C distances; pC-O & pCo-C=C-O & single Co-C bond orders; BE=binding energy; vC-O & vCo-C=C-O & Co-C stretching frequencies; T=on-top site, B=2-fold bridge site; Numbers in parenthesis indicate Co atoms involved in each site and position; Superscripted t=on top layer, m=on middle layer.

ever, there were no vital differences in those computed values between these two hollow sites, implying little effect of Co atoms of the middle layer, which is 2.0494 Å below the top layer and too distant to affect the CO adsorption on the top layer.

CO Bindings on Co(10 $\bar{1}0$), (11 $\bar{2}0$), and (10 $\bar{1}2$). The Co₄₃(10 $\bar{1}0$) cluster surface (in Figure 3) affords two binding sites, on-top and 2-fold bridge, and these are available on two layers, top or middle. In Table 5, there were exposed steady increases in the C-O and Co-C distances with the matching decreases in the C-O and Co-C bond orders, and also increments in the binding energy (BE) of single CO's on the CO site proceeding from on-top to 2-fold bridge, of either top or middle layer. Of the top layer, dC-O and dCo-C ranged from 1.110-1.112 Å and 1.744-1.754 Å for on-top site to 1.122-1.122 Å and 1.882-1.887 Å for bridge site, respectively, while their pC-O and pCo-C spanned from 1.51-1.52 and 0.81-0.86 to 1.48 and 0.45-0.47, each, for such sites. Binding energies also slightly escalated from 3.14-3.48 eV for on-top to 3.57-3.88 eV for bridge site CO molecules. The changes of these values on the middle layer, indicated as superscripted m in Table 5, paralleled those on the top layer.

By an argument similar to that on the (0001), overall binding energies of single CO on the (10 $\bar{1}0$) surface (3.15-3.99 eV) were appraised quite larger than an isosteric heat of adsorption, 1.48 eV, on the same (10 $\bar{1}0$) measured by Papp.³¹ However, the slight largeness in the BE range for on-top CO's on the (10 $\bar{1}0$) (3.14-3.48 eV) compared to that on the (0001) (2.96-3.32 eV) resembled closely the situation in Papp's experiment; 1.48 eV on the (10 $\bar{1}0$) and 1.33 eV on the (0001). It is noted that pCo-C values for 2-fold bridge CO on the middle layer, *i.e.*, B(18,19)^m, are indeed due to contributions from four individual Co-C overlap populations, two major overlaps between a carbon and two middle Co atoms (# 18

Table 6. The results from CO on $\text{Co}_{49}(11\bar{2}0)$ cluster surface

Site & position	dC-O (Å)	dCo-C (Å)	pC-O	pCo-C	BE (eV)	vC-O (cm^{-1})	vCo-C (cm^{-1})
T(1) ^y	1.109	1.747	1.52	0.84	-3.42	1932	590
T(2) ^y	1.110	1.748	1.50	0.85	-3.43	1953	585
T(9) ^y	1.110	1.758	1.52	0.77	-3.07	1961	574
T(10) ^y	1.111	1.753	1.52	0.79	-3.19	1949	581
T(20) ^m	1.113	1.849	1.57	0.63	-3.84	1880	468
T(22) ^m	1.115	1.850	1.56	0.63	-3.63	1853	471
T(27) ^m	1.108	1.830	1.59	0.68	-3.59	1846	483
B(1,2) ^y	1.127	1.880	1.46	0.47	-3.83	1705	495
B(2,10) ^y	1.125	1.887	1.47	0.46	-3.55	1732	486
B(8,9) ^y	1.121	1.895	1.48	0.44	-3.25	1772	472
B(1,3) ^m	1.129	1.933	1.51	0.39	-3.60	1667	271
B(4,12) ^m	1.128	1.944	1.51	0.38	-3.49	1686	283

dC-O & dCo-C=C-O & Co-C distances; pC-O & pCo-C=C-O & single Co-C bond orders; BE=binding energy; vC-O & vCo-C=C-O & Co-C stretching frequencies; T=on-top site, B=2-fold bridge site; Numbers in parenthesis indicate Co atoms involved in each site and position; Superscripted t=on top layer, m=on middle layer.

and #19) bound strongly to the CO, and two minor overlaps between the carbon atom and two top Co atoms (#1 and #3) bound weakly to the CO.

On-top and 2-fold bridge site (of top or middle layer) are available for the adsorption of a CO on the zigzag $\text{Co}_{49}(11\bar{2}0)$ cluster surface (see Figure 4). Table 6 exhibits that the site shift of CO from on-top to 2-fold bridge (either of the top or middle layer) causes slight increases in the dC-O. Of the top layer, the C-O bond weakened scarcely from 1.109-1.111 Å to 1.121-1.127 Å with the resulting reductions in the pC-O from 1.50-1.52 to 1.46-1.48, and the Co-C bond also loosened for that CO site shift (see gains in the dCo-C from 1.747-1.758 Å to 1.880-1.895 Å and losses in the pCo-C from 0.77-0.79 to 0.44-0.47). Binding energies (BE) of bridge site CO species (3.25-3.83 eV) were larger than those of on-top ones (3.07-3.42 eV) of the top layer. Of the middle layer, the changing fashion of these values on shifting from on-top to bridge CO site were close to that on the top layer. But, binding energies for on-top site CO's on the middle layer, e.g., T(20)^m, were estimated somewhat larger, considering their low Co-C bond orders. The cause for this could be due to some contribution from nearby top Co atoms (#1, #2, #6, and #7) to the Co-C bond orders.

There are available two sites, on-top (of top, middle, or bottom layer) and 2-fold bridge (of middle or bottom layer) of a CO on the $\text{Co}_7(10\bar{1}2)$ (see Figure 5). As shown in Table 7, both C-O and Co-C bonds enlarged from 1.106-1.110 Å and 1.758-1.764 Å for on-top to 1.121-1.123 Å and 1.884-1.890 Å for bridge CO species, respectively, of the top layer with the succeeding drops in the pC-O from 1.52-1.54 to 1.47-1.48 and in the pCo-C from 0.79-0.81 to 0.44-0.46, analogous to the previous Co(0001), (10 $\bar{1}0$), and (11 $\bar{2}0$) planes. Calculated binding energies (BE) on the (10 $\bar{1}2$) exhibit the more strong

binding of a CO to the surface by bridges over on-top sites. These values for CO on the middle layer showed little difference from those on the top layer as foreseen, considering small layer-layer separation; the middle layer is only 0.4970 Å below the top layer. However, on-top CO sites of the bottom layer which is 2.5100 Å below the top layer, i.e., T(42)^y, are not entirely on-tops, but have some contributions (nearly 0.10 each) to the pCo-C between the carbon and #42 Co atom from two nearest top Co atoms (for example, #8 and #9) and so bare slightly larger BE values.

The development of atomic charges on carbon and oxygen of CO by adsorption on these three cobalt surfaces, (10 $\bar{1}0$), (11 $\bar{2}0$), and (10 $\bar{1}2$) was alike to the (0001), as shown in Table 4. The site change of CO binding from on-top to multiple bridges on these surfaces led to less positively charged carbon and more negatively charged oxygen atoms. So, more highly and negatively charged CO molecules by bridge sites will repel more each other and become less stable at high CO coverage. Tilted (or inclined) bridge or hollow sites on the Co (10 $\bar{1}0$) or (11 $\bar{2}0$), even tilted 4-fold bridge site on the (10 $\bar{1}2$), seem to be likely, but they are not dealt with in this paper, since only binding sites of CO with the C-O axis perpendicular to the surface are considered in this paper. However, these tilted sites on cobalt surfaces will be an interesting topic for future studies.

C-O and Metal-C Vibrational Frequencies

CO Vibration on Co(0001). From the results for single CO molecules on the $\text{Co}_{50}(0001)$ (in the last two columns of Table 3), it is observed that stretching C-O vibrational frequencies (vC-O) decrease significantly from 1969-1992 cm^{-1} for on-top to 1693-1763 cm^{-1} for 2-fold bridge and then to 1560-1635 cm^{-1} for 3-fold hollow site CO species. The corresponding Co-C stretching frequencies (vCo-C) also declined, but not as strongly as the vC-O, from 582-594 cm^{-1} to 492-508 cm^{-1} and to 470-482 cm^{-1} for that CO site change. These trends of changes in the C-O and metal-C vibrational frequencies due to different CO sites have been reported in several experiments^{32,33} and also in calculation works^{14,27} on other metal crystal surfaces. For a particular example, Maruca *et al.*¹⁴ reported the calculated vC-O values from CO on a Ni (111), which is very like in the surface geometry to a Co(0001), as follows: 2071-2080 cm^{-1} for on-top, 1835-1860 cm^{-1} for 2-fold bridge, and 1707-1750 cm^{-1} for 3-fold hollow site CO species.

Vibrational spectra for CO molecules on cobalt crystal surfaces were rarely obtained in experiment. EELS spectra of CO on a cobalt (0001) from an experiment by Geerlings *et al.*²⁶ showed 1990 cm^{-1} for the stretching C-O frequency and 500 cm^{-1} for the corresponding Co-C frequency. This experimental vC-O value (1990 cm^{-1}) was in fact chosen as a reference in this calculation work to further calibrate the valence state ionization energy of cobalt 3d orbitals, VSIE_{3d}. In Raman spectra obtained for CO gases on a polycrystalline cobalt, Marzouk *et al.*³⁴ obtained the observed C-O and Co-C frequency ranges as follows; 2033-2118 cm^{-1} and 456-525 cm^{-1} for linear on-top, 1838-2010 cm^{-1} for 2-fold bridge, and 1750-1818 cm^{-1} and 260-305 cm^{-1} for 3-fold bridge CO species, each. The changing tendencies of these values for the on-top to multiple site change agreed with our calculation, whereas overall vC-O frequencies were higher than our val-

ues. However, compared to their observation; increase in the $\nu\text{C-O}$ and decrease in the matching $\nu\text{Co-C}$ for different positions and environments of CO on a given specific site (e.g., on-top), our calculation results on the (0001) indicated that $\nu\text{Co-C}$ increases always as $\nu\text{C-O}$ increases in different positions of an on-top site CO (see the results from #1, #2, and #9 positions of on-top site in Table 3). Also, there was little difference between the $\nu\text{C-O}$ range (2033-2118 cm^{-1}) reported for CO on a poly Co surface and that (2036-2110 cm^{-1}) for their similar work, CO on a Ni (111),³⁵ with no clear discussion.

CO Vibrations on Co(10 $\bar{1}$ 0), (11 $\bar{2}$ 0), and (10 $\bar{1}$ 2).

Stretching C-O and Co-C vibrational frequencies on other cobalt crystalline planes; Co(10 $\bar{1}$ 0), (11 $\bar{2}$ 0), and (10 $\bar{1}$ 2) varied with the same fashion as on the (0001) for the CO site shift of on-top to bridges; significant decrease in the $\nu\text{C-O}$ and moderate drop in the $\nu\text{Co-C}$.

On the Co(10 $\bar{1}$ 0), C-O stretching frequency descended markedly from 1923-1954 cm^{-1} for on-top to 1756-1777 cm^{-1} for bridge site CO species, while the corresponding Co-C frequency downed from 583-598 cm^{-1} to 489-493 cm^{-1} (see Table 5). For the Co(11 $\bar{2}$ 0), $\nu\text{C-O}$ and $\nu\text{Co-C}$ values shifted down from 1932-1961 cm^{-1} and 574-590 cm^{-1} for on-top to 1705-1772 cm^{-1} and 472-495 cm^{-1} for bridge CO species, respectively (in Table 6). Likely, on the Co(10 $\bar{1}$ 2), $\nu\text{C-O}$ and $\nu\text{Co-C}$ diminished from 1980-1987 cm^{-1} and 569-577 cm^{-1} for on-top to 1757-1792 cm^{-1} and 485-491 cm^{-1} for bridge CO's (Table 7). These results are all for the top layer of each surface. The results on the middle layer showed the same trend.

As discussed above, on all cobalt surfaces, stretching C-O frequencies always decrease with their decreased C-O bond orders for the CO site change from on-top to bridge and/or to hollow on a specific layer. However, there were some opposite (unpredicted) circumstances in case of the layer to layer shift of a given particular CO site. For example, on the (10 $\bar{1}$ 2), $\nu\text{C-O}$ frequencies drop considerably for the layer shift from the top (*i.e.* 1987 cm^{-1} at #8) or middle (*i.e.* 1979 cm^{-1} at #28) of an on-top site CO to the bottom layer (*i.e.* 1912 cm^{-1} at #42), while their $\nu\text{Co-C}$ values increase from 1.54 or 1.53 to 1.60. This could be explained by dragging (or sticking) effect of nearby cobalt atoms on a carbon atom. That is, two top Co atoms (#8 and #9) which separate 2.06 Å each from the C atom of an on-top site CO (#42) on the bottom layer and interfere with the stretching motion of the C atom by dragging. The dragging will cause the similar effect as increase in the carbon mass, increase in the reduced mass of CO, and so decrease in the C-O stretching frequency, but with little effect on the force constant of CO. These effects are also observed for an on-top CO (e.g., #20) or 2-fold bridge CO (e.g., #(19,22)) of the middle layer on the Co(11 $\bar{2}$ 0) surface.

Geerlings *et al.* showed 1980 cm^{-1} for the stretching C-O frequency and 440 cm^{-1} for the corresponding Co-C frequency on the Co(10 $\bar{1}$ 2) surface in a recent experiment.³⁶ Our calculated $\nu\text{C-O}$ values (1980-1987 cm^{-1}) for on-top site CO on the (10 $\bar{1}$ 2) seem very close to their experimental value (1980 cm^{-1}). In addition, for an on-top CO (of the center), a slight decrease in the $\nu\text{C-O}$ from 1992 cm^{-1} on the (0001) to 1987 cm^{-1} on the (10 $\bar{1}$ 2) resembled the circumstance from Geerlings *et al.*; 1990 cm^{-1} on the (0001)³⁶ and 1980 cm^{-1}

Table 7. The results from CO on Co₄₇(10 $\bar{1}$ 2) cluster surface

Site & position	dC-O (Å)	dCo-C (Å)	pC-O	pCo-C	BE (eV)	$\nu\text{C-O}$ (cm^{-1})	$\nu\text{Co-C}$ (cm^{-1})
T(8) ^y	1.106	1.758	1.54	0.81	-3.29	1987	577
T(13) ^y	1.105	1.759	1.55	0.80	-3.29	1999	574
T(18) ^y	1.109	1.758	1.52	0.83	-3.37	1979	577
T(20) ^y	1.110	1.764	1.52	0.80	-3.14	1980	569
T(28) ^m	1.108	1.754	1.53	0.86	-3.38	1979	587
T(33) ^m	1.109	1.757	1.53	0.84	-3.32	1975	582
T(35) ^m	1.108	1.763	1.53	0.81	-3.21	1997	574
T(42) ^y	1.109	2.383	1.60	0.82	-3.46	1912	382
T(43) ^y	1.110	2.391	1.60	0.79	-3.43	1911	373
B(8,9) ^y	1.123	1.884	1.47	0.46	-3.82	1757	491
B(9,10) ^y	1.121	1.890	1.48	0.44	-3.66	1792	485
B(28,29) ^m	1.125	1.886	1.46	0.48	-3.85	1759	493
B(34,35) ^m	1.122	1.904	1.48	0.45	-3.65	1793	486

dC-O & dCo-C=C-O & Co-C distances; pC-O & pCo-C=C-O & single Co-C bond orders; BE=binding energy; $\nu\text{C-O}$ & $\nu\text{Co-C}$ =C-O & Co-C stretching frequencies; T=on-top site, B=2-fold bridge site; Numbers in parenthesis indicate Co atoms involved in each site and position; Superscripted t=on top layer, m=on middle layer.

on the (10 $\bar{1}$ 2).³⁶

Carbon Atom Vibrations on Cobalt Surfaces

Though no identified stretching frequencies have yet been reported for atomic carbon on cobalt surfaces, these atomic C-Co stretching frequencies were computed in the present study as a possible aid in a future experiment. The results are summarized in short as follows: 1009-1045 cm^{-1} for on-top, 720-769 cm^{-1} for bridge, and 644-686 cm^{-1} for hollow site carbon on the Co(0001); 1049-1060 cm^{-1} and 732-784 cm^{-1} on the (10 $\bar{1}$ 0), 1038-1047 cm^{-1} and 775-801 cm^{-1} on the (11 $\bar{2}$ 0), and 1057-1074 cm^{-1} and 729-787 cm^{-1} on the (10 $\bar{1}$ 2) for on-top and bridge carbon, respectively. These values were calculated all for the top layer.

Conclusion

The binding structure, energetics, and vibrational frequencies of single CO molecules adsorbed on cobalt crystal surfaces: Co₅₀(0001), Co₄₃(10 $\bar{1}$ 0), Co₄₅(11 $\bar{2}$ 0), and Co₄₇(10 $\bar{1}$ 2) were investigated theoretically in this study employing the semi-empirical ASED-MO method as a preceding study for the interaction (mainly CO dissociation and carbon aggregation) of CO molecules on these cobalt surfaces and also to help better understand the mechanism for CO dissociation on these cobalt surfaces.

On the Co(0001) surface, there were observed gradual increases in the C-O and corresponding Co-C distances (dC-O and dCo-C), together with the consequent decreases in the C-O and Co-C bond orders (pC-O and pCo-C), as the binding site of CO changes from on-top (linear) to 2-fold bridge and then to 3-fold bridge (or hollow) sites. Calculated

binding energies (BE) indicated that single CO molecules are more strongly bonded, with larger BE values, to the surface by multiple bridge sites. That is, 3-fold bridge CO species become most stable, 2-fold bridge species next most stable, and on-top ones least stable.

Atomic charges developed on carbon and oxygen lead to more highly and negatively charged multiple bridge site CO, forcing nearby CO molecules to repel more with each other, which will make multiple site CO species less stable at high CO coverages. This could account for experimental observation that multiple bridge site CO molecules become less stable as the CO coverage increases. Among different positions of CO for a given specific site and layer, there has been detected size (edge) effect which will disappear with the infinite size of a cobalt cluster.

On the Co(10 $\bar{1}$ 0), (11 $\bar{2}$ 0), and (10 $\bar{1}$ 2), the results were similar to that on the (0001); there were exposed steady increases in the dC-O and dCo-C with the consequent declines in the pC-O and pCo-C, additions in binding energy and relative stability of a CO, and developing of more negative charges on whole CO as the binding site shifts from on-top to multiple bridges.

On all cobalt surfaces, stretching C-O vibrational frequencies (ν C-O) decreased significantly by the site change of CO from on-top to multiple bridges and the corresponding Co-C frequencies (ν Co-C) also downed, but not as strongly as the ν C-O. These changing trends in the ν C-O and ν Co-C for different CO binding sites were analogous to those reported in experiment and theoretical calculation. There were trivial size effects, small variations in the ν C-O and ν Co-C among different positions of CO within a given particular site and layer.

Atomic stretching C-Co frequencies were computed in our study as a possible aid in future experiments while no identified stretching frequencies for atomic carbon on cobalt surfaces have been reported.

Acknowledgment. We gratefully acknowledge a generous amount of free computer time on the University of Kentucky IBM 3090-300E Supercomputer through the completion of this work.

References

- Kelly, P. D.; Goodman, D. W. In *The Chemical Physics of Solid Surfaces and Heterogeneous Catalysis*; King, D. A.; Woodruff, D. P., Ed.; Elsevier: New York, U.S.A., 1982; Vol. 4, p 427.
- Boudart, M.; McDonald, M. A. *J. Phys. Chem.* 1984, 88, 2185.
- Nakamura, J.; Toyoshima, I.; Tanaka, K. *Surf. Sci.* 1988, 201, 185.
- Goodman, D. W. *Acc. Chem. Res.* 1984, 17, 194.
- Blyholder, G. *J. Phys. Chem.* 1964, 168, 2772.
- Ray, N. K.; Anderson, A. B. *Surf. Sci.* 1982, 119, 35.
- Ishi, S.; Ohno, Y.; Viswanathan, B. *Surf. Sci.* 1985, 161, 349.
- Steininger, H.; Lehwald, S.; Ibach, H. *Surf. Sci.* 1982, 123, 264.
- Bare, S. R.; Hofmann, P.; King, D. A. *Surf. Sci.* 1984, 144, 347.
- Shinn, N. D.; Madey, T. E. *J. Chem. Phys.* 1985, 83, 5928.
- Mehandru, S. P.; Anderson, A. B. *Surf. Sci.* 1988, 201, 345.
- Sheppard, N.; Nguyen, T. T. In *Advances in Infrared and Raman Spectroscopy*; Clark, R. J. H.; Hester, R. E., Ed.; Heyden: London, U. K., 1978; Vol. 5, p 67.
- Biberian, J. P.; Van Hove, M. A. *Surf. Sci.* 1984, 138, 361.
- Maruca, R.; Kusuma, T.; Hicks, V.; Companion, A. *Surf. Sci.* 1990, 236, 210.
- Goodman, D. W.; Kelly, R. D.; Madey, T. E.; Yates, Y. T. *J. Catal.* 1980, 63, 226.
- Anderson, A. B. *J. Chem. Phys.* 1974, 60, 2477.
- Anderson, A. B.; Hoffmann, R. *J. Chem. Phys.* 1974, 60, 4271.
- Hicks, V., unpublished work, 1988.
- Huff, N. T.; Ellison, F. O. *J. Chem. Phys.* 1965, 42, 364.
- Rosen, B. *Spectroscopic Data Relative to Diatomic Molecules*; Pergamon: Oxford, U. K., 1970; p 98.
- Huber, K. P.; Herzberg, G. *Molecular Spectra and Molecular Structure*; Van Nostrand-Reinhold: New York, U.S.A., 1979; p 158.
- Penner, S. S.; Weber, J. D. *J. Chem. Phys.* 1951, 19, 807.
- McClellan, A. D. *Table of Experimental Dipole Moments*; Freeman: San Francisco, U.S.A., 1963; p 48.
- Nichols, J. F. *An Atlas of Models of Crystal Surfaces*; Gordon and Breach: New York, U.S.A., 1965; p 45.
- Kittel, C. *Introduction to Solid State Physics*; Wiley: New York, U.S.A., 1986; p 59.
- Geerlings, J. J. C.; Zonneville, M. C.; de Groot, C. P. M. *Surf. Sci.* 1991, 241, 302.
- Jörg, H.; Rösch, N. *Surf. Sci.* 1985, 163, L627.
- Rosen, A.; Baerends, E. J.; Ellis, D. E. *Surf. Sci.* 1979, 82, 139.
- Papp, H. *Surf. Sci.* 1983, 129, 205.
- Tracy, J. C. *J. Chem. Phys.* 1972, 56, 2736.
- Papp, H. *Ber. Bunsenges. Physik. Chem.* 1982, 86, 555.
- Bertolini, J. C.; Tardy, B. *Surf. Sci.* 1981, 102, 131.
- Campuzano, J. C.; Greenler, R. G. *Surf. Sci.* 1979, 83, 301.
- Marzouk, H. A.; Bradley, E. B.; Arunkumar, K. A. *Spectrosc. Lett.* 1985, 18, 189.
- Marzouk, H. A.; Arunkumar, K. A.; Bradley, E. B. *Surf. Sci.* 1984, 147, 477.
- Geerlings, J. J. C.; Zonneville, M. C.; de Groot, C. P. M. *Surf. Sci.* 1991, 241, 315.